

Energy-based damage assessment of continuous-span reinforced concrete highway bridges

S. Mahboubi[†] and M. R. Shiravand[‡]

Faculty of Civil, Water and Environmental Engineering, Shahid Beheshti University, Tehran 1658953571, Iran

Abstract: This paper conducts a comparative study on seismic damage to reinforced concrete (RC) bridges, using three damage models: Park and Ang, Hindi and Sexsmith, and input energy-based damage (IEBD) indices, and presents a global cumulative damage model based on the IEBD index to establish a practical damage assessment of an overall bridge system. A series of RC bridges are studied under seismic loadings, and to compare the efficiency and reliability of the damage indices, damage curves of RC piers are developed, and damage levels of piers are calculated at design basis earthquake (DBE) and maximum considered earthquake (MCE) levels. The global cumulative damage index is calculated for bridge models regarding damage values of components. The results indicate that the IEBD index shows a gradual progression of damage and provides reasonable values for different damage levels of piers compared to two other damage indices. Moreover, the global cumulative damage index shows the impact of induced damage to a certain component regarding the damage level of the overall bridge system. Moreover, this new approach is a relatively simple and practical tool for seismic damage assessment of RC bridge systems, which can be implemented in finite element models, particularly in the absence of experimental data.

Keywords: RC bridge; energy-based damage index; global cumulative damage index; IEBD Index

1 Introduction

Quantitative assessment of seismic damage to reinforced concrete (RC) bridges is crucial for performance-based design of bridge structures. Recent earthquakes reveal that the seismic response of an overall bridge system depends predominately on its component behavior. Therefore, the evolution from the component to system damage and a definition of bridge damage in terms of quantitative component damage levels is required for seismic assessment of bridge structures. The most common type of damage observed in RC bridges during earthquakes are flexural- and shear deformation-induced damage to RC piers and the unseating of bridge spans, bearings and abutment damages. However, insufficient resistance and the low ductility capacity of bridge columns are the main failure modes of RC bridges that lead to severe damage during recent earthquakes (Jara *et al.*, 2014). In damage assessment studies, seismic damage to RC bridges has been generally related to engineering demand parameters such as the plastic rotation of RC piers, lateral displacement, and drift and ductility with damage

indices. Damage indices are structural parameters that have been used for representing a level of damage to a quantifiable degree. The suitability of a chosen structural parameter as a damage index depends on the failure modes of structures. Deformation-based damage indices, which relate damage to the maximum response of a structural system, are the most widely used model in seismic vulnerability studies regarding the conceptual simplicity of using peak response as a damage criterion (Mahboubi and Shiravand, 2019). Many researchers have utilized non-cumulative damage indices like drift and ductility for seismic damage assessment of RC bridges. For example, Nielson and DesRoches (2007) developed fragility curves for nine RC bridge classes that are common to the central and southeastern United States, using curvature ductility and deformation limits for bridge columns and bearings, respectively. Padgett *et al.* (2008) utilized ductility as a damage index to perform probabilistic analyses for determining optimal seismic intensity measures when generating probabilistic seismic demands for bridges. Babazadeh *et al.* (2015) defined damage limit states for RC bridge columns based on displacement ductility to conduct finite element analysis. Goodnight *et al.* (2019) used strain and displacement ductility of RC bridge piers as the damage index and carried out experimental and numerical studies on thirty large-scale RC bridge columns that were subjected to reversed cyclic loading and seismic load histories. However, experimental studies show that structural materials experience stiffness and strength degradation during repeated loading cycles. Therefore,

Correspondence to: M. R. Shiravand, Faculty of Civil, Water and Environmental Engineering, Shahid Beheshti University, Tehran 1658953571, Iran
Tel: +98-2173932439
E-mail: m_shiravand@sbu.ac.ir

[†]PhD; [‡]Associate Professor

Received February 11, 2021; Accepted July 15, 2022

the level of imposed damage strongly depends on the number of loading cycles and past loading history (Krawinkler and Zohrei, 1983; Chai and Romstad, 1995; Mander *et al.*, 1994; El-Bahy *et al.*, 1999; Banerjee and Shinozuka, 2008; Guo *et al.*, 2016; Sun *et al.*, 2017; Shiravand and Rasouli, 2019; Seyed Ardakani *et al.*, 2021; Mahboubi and Kioumars, 2021). These efforts highlight the need to shift from non-cumulative deformation-based damage parameters to cumulative damage indices in seismic design and analysis. The concept of energy seems the best approach to describe structural damage due to earthquake excitement, and energy-based damage indices have been effectively used in seismic response evaluation of structural systems. The energy-based damage models relate seismic induced damage to the energy dissipation capacity of a structural system and consider earthquake effects on the system as a function of the structural properties and characteristics of ground motion or earthquake input energy. This fact led researchers to use the concept of energy in damage indices (Park and Ang, 1985; Hindi and Sexsmith, 2001; Erberik and Sucuoğlu, 2004).

Using damage indices for damage evaluation of bridges appears to have been favored in many previous experimental and analytical studies (Kunnath *et al.*, 1997; Hachem *et al.*, 2003; Calvi *et al.*, 2005; Iranmanesh and Ansari, 2014). Lehman and Moehle (2000) proposed a dual-phase damage index to characterize the seismic performance of modern bridge columns. The damage index was examined through experimental and analytical investigations conducted for different damage states. Hindi and Sexsmith (2004) assessed seismic damage distribution in the RC piers of two bridges in Canada, using their proposed energy-based damage index. Bassam *et al.* (2011) developed the displacement-based damage index proposed by Powell and Allahabadi (1998) to consider the effects of low-cycle fatigue on lateral displacements of bridge piers. They also used that methodology for a damage investigation of a four-span bridge subjected to progressively greater ground motions. Cardone (2014) suggested some deformation-based damage indices for bridge components, including piers, abutments, shear keys and bearings. Jara *et al.* (2014) used a damage index proposed by the Park and Ang (1985) for the seismic assessment of RC bridges in Mexico. The plastic pier rotations and the spectral acceleration of the fundamental period of a specific bridge was chosen as the engineering demand parameters and intensity measures, respectively. Roy *et al.* (2017) evolved the Park and Ang (1985) damage index to assess the maximum credible damage of RC bridge piers subjected to bi-directional seismic excitations. Oskoui *et al.* (2019) presented a damage index for identifying micro-crack locations along the spans of continuous bridges and evaluated the model by testing a five-span box-girder bridge. Mahboubi and Shiravand (2019b) performed a comparative study to quantify the seismic damage of skew RC bridge piers retrofitted with carbon

fiber reinforced polymer (CFRP), using displacement-, energy- and stiffness-based damage models. In other studies done by Mahboubi and Shiravand (2019a, c) the authors proposed an energy-based damage index for the damage assessment of RC bridge components such as piers and bearings, using the concept of energy balance laws within a structural system. The damage index was defined as the ratio of hysteretic energy to the external work done by a system. The authors examined the proposed energy-based damage index through verification studies conducted on RC piers and bearings. They also presented damage classifications for RC columns and bearings with respect to the constitutive material models and structural failure modes, based on experimental and fiber-based analyses. A summary of the most used damage indices in the seismic assessment of bridges is shown in Table 1.

Most of the existing performance-based studies have used damage indices solely for bridge columns, whereas the lateral responses and the energy dissipation capacity of a bridge system depends to a great extent on the inelastic behavior of columns and the energy dissipation capacity of other components like bearings, abutments, and shear keys. In addition, there is no study on a global cumulative damage index that can represent deterioration of a bridge system to a quantifiable degree, based on an energy-based damage model with respect to damage measures of its components. The overarching aim of this paper is to perform a comparative study on three damage indices, which utilizes the concept of energy while presenting a global damage index for the damage assessment of an RC bridge system using its component damage models. For this purpose, the damage curves of a series of RC bridges with different configurations are developed using the Park and Ang (1985), Hindi and Sexsmith (2001) and IEBD index proposed by Mahboubi and Shiravand (2019a). Moreover, a global cumulative damage index is presented as a function of component damage measures, incorporating weight coefficients for quantifying the level of damage to a bridge system throughout its loading history. The damage values of each bridge component are calculated using the IEBD index, and the damage values of the overall bridge systems are calculated by employing the global cumulative damage index.

2 Damage indices

Park and Ang (1985) defined a damage index as a linear function of the ductility and cumulative hysteretic energy demand, as represented below:

$$DI = \frac{\delta_m}{\delta_u} + \frac{\beta}{Q_y \delta_u} \int dE \quad (1)$$

where δ_m is maximum deformation, δ_u is the ultimate deformation capacity under monotonic loading, Q_y is

Table 1 Damage index in seismic damage analysis of bridges art review

Damage Index	Bridge Component	Damage Parameters	Proposed by
$D = \frac{k_m - k_0}{k_f - k_0}$	Columns	Stiffness	Kunnath <i>et al.</i> (1997)
$D_{pA} = \frac{\delta_m}{\delta_u} + \frac{\beta}{Q_u \delta_u} \int dE$	Columns	Ductility and Energy	Park and Ang (1985)
$(N_f)_c = 33 \left(\frac{\epsilon_c}{\epsilon_{csp}} \right)^{-5}$	Columns	Strain	Lehman and Moehle (2000)
$(N_f)_s = 0.08 \left(\frac{\epsilon_s}{\epsilon_{su}} \right)^{-5.5} + 0.92$	Columns	Low-Fatigue	Lehman and Moehle (2000)
$D_n = \left(\frac{A_0 - A_n}{A_0} \right)$	Columns	Energy	Hindi and Sexsmith (2001)
$DI = \frac{\delta_m}{\delta_u} + \frac{\delta_m}{\delta_u} \left(\frac{1}{FD} - 1 \right)$	Columns	Ductility	Bassam <i>et al.</i> (2011)
$DI = \alpha d_y + \beta (d_u - d_y)$	Piers, abutments, shear keys and bearings.	Displacement	Cardone (2014)
$DI = \frac{E_h}{E_p} = 1 - \frac{E_k + E_d + E_s}{E_p}$	Columns and Bearings	Energy	Mahboubi and Shiravand (2019a)

the yield strength, E is the absorbed hysteretic energy and β is a parameter that depends on the structural characteristics of the RC member and considers the effect of cyclic loading that is mostly determined by experiments or through an empirical expression, namely:

$$\beta = (-0.447 + 0.073 \frac{l}{d} + 0.24 \frac{P}{f'_c b d} + 0.31 \rho_1) 0.7^{\rho_s} \quad (2)$$

where $\frac{l}{d}$ is shear span ratio and ρ_1 and ρ_s are the percentage of the longitudinal and transverse steel ratios, respectively. The damage classification presented by Park and Ang (1985) is shown in Table 1.

Hindi and Sexsmith (2001) presented an energy-based damage index regarding the hysteretic behavior of a concrete column and the work needed to fail a RC column under monotonic loading, as shown below:

$$DI = \frac{(A_0 - A_n)}{A_0} \quad (3)$$

where A_0 is the energy under a monotonic load-displacement curve up to the point of failure and A_n is the global energy for the damage state, which is defined as the energy under a monotonic load-displacement curve from the end of the last cycle n (zero force point) to failure. The Hindi and Sexsmith (2001) damage states are listed in Table 3.

The IEBD proposed by Mahboubi and Shiravand (2019a, c) can be used to estimate the damage levels of a structure subjected to cyclic/seismic loading throughout loading protocol/histories. The proposed damage index is defined as the ratio of hysteretic energy, (E_h) to the

input energy to the system due to external forces (E_p). For a structural system, the damage index is expressed by:

$$DI = \frac{E_h}{E_p} \quad (4)$$

The balance between input energy due to external forces and the absorbed energy provides a simple approach for understanding the behavior of a structural system up to failure. When a structure is subjected to earthquake excitements, the external work of the structure during seismic loadings can be represented by earthquake input energy, which is distributed within the structure in the form of kinetic energy (E_k), inherent damping energy (E_d), strain energy (E_s), and hysteretic energy. Considering the energy balance equation for a system, Mahboubi and Shiravand (2019a) suggested that the hysteretic energy in the proposed damage index can be calculated using the difference between input energy to the system due to external forces and other energy components, as expressed in Eq. (5):

$$E_h = E_p - E_k - E_d - E_s \quad (5)$$

Therefore, Eq. (4) can be expressed by:

$$DI = \frac{E_h}{E_p} = 1 - \frac{E_k + E_d + E_s}{E_p} \quad (6)$$

According to Eq. (6), the IEBD index presents a new idea, namely, that input energy to the system due to external forces can be used for damage evaluation rather than considering the loading effects as functions of

structural parameters. Input energy due to an earthquake can reflect the general characteristics of earthquakes, such as amplitude, duration, and frequency at each time point throughout their duration. In addition, the effects of seismic loads on a system can be explained not as force or displacement independently, but rather as the product of both in terms of the external work. Therefore, the IEBD index considers earthquake effects on the system in a more realistic way. Moreover, the energy dissipation in this damage model reflects the characteristics of the inelastic behavior of a system and is calculated using the difference between the input energy and other energy components to ensure that all cumulative effects of loading are considered for each cycle.

Mahboubi and Shiravand (2019a) presented a damage classification for RC bridge piers based on the IEBD index regarding the proposed strain-based damage levels (Table 4). The authors suggested strain-based damage levels for RC columns with respect to the steel and concrete constitutive material models and conducted a series of verification studies on flexural/shear-dominated RC bridge columns under cyclic and seismic loadings. In addition, in another study by the same authors (Mahboubi and Shiravand, 2019c) suggested damage levels for three commonly used bridge bearings (Table 5), using the IEBD index, based on calibration studies they did on a series of experimental specimens subjected to different cyclic and seismic loading protocols (Mahboubi and Shiravand, 2019a).

As observed in Tables 2–5, according to the Hindi and Sexsmith (2001) and IEBD models, $DI \leq 1$ indicates no damage to RC bridge piers, whereas in the case of

the Park and Ang (1985) damage index, this range of DI corresponds to localized minor cracking. Moreover, the Park and Ang (1985) damage value index, between 0.1–0.25, represents light cracking throughout the piers. In the case of the Hindi and Sexsmith (2001) and IEBD models, damage values between 0.1–0.2 are correlated to light cracking of concrete and the first yield of steel reinforcement. Severe cover cracking and spalling have been considered to be moderate damage levels by all three defined damage models. The Park and Ang (1985) damage values, in a range between 0.4–1, have been defined as severe/extensive damage correlated to concrete crushing and exposed reinforcement. On the other hand, the Hindi and Sexsmith (2001) damage model defined damage values between 0.4–0.6 for extensive cracking and exposed reinforcement, and damage measures between 0.6–1 for concrete crushing and bar buckling. Moreover, the IEBD index considered $0.7 \leq DI < 0.9$, as the extensive damage level corresponding to bar buckling in RC piers. The complete damage level is correlated to collapse according to the Park and Ang (1985) and Hindi and Sexsmith (2001) damage models, where $DI \geq 1$ and $DI = 1$, respectively. In contrast, the IEBD index considered core concrete crushing as the complete damage limit that is correlated to a damage value between 0.9–1.

Note that to examine the damage indices by considering their conditions and properties, the authors have calculated these damage indices for five experimental specimens and compared the results with the damage states reported through experimental studies (Mahboubi and Shiravand, 2019a).

Table 2 Park and Ang (1985) damage limit states

Damage state	Damage description	Damage index
No damage	Localized minor cracking	$DI < 0.1$
Minor	Light cracking throughout	$0.1 \leq DI < 0.25$
Moderate	Severe cracking, localized spalling	$0.25 \leq DI < 0.4$
Severe	Concrete crushing, reinforcement exposed	$0.4 \leq DI < 1$
Complete	Collapse	$DI \geq 1$

Table 3 Hindi and Sexsmith (2001) damage states

Damage state	Damage description	Damage index
No damage	No damage	$DI < 0.1$
Minor	Light cracking-very easy to repair	$0.1 \leq DI < 0.2$
Moderate	Severe cracking, cover spalling, repairable	$0.2 \leq DI < 0.4$
Severe	Extensive cracking, reinforcement exposed, repairable with difficulties	$0.4 \leq DI < 0.6$
Severe	Severe damage-concrete crushing, reinforcement buckling, irreparable	$0.6 \leq DI < 1$
Complete	Collapse	$DI = 1$

3 Global energy-based damage index

Damage to components may result in different damage levels for the overall bridge system. Hence, a damage index is required to estimate the measure of the damage sustained by the bridge system as a function of component damage values. A suitable damage index should show the distribution of damage occurring throughout a bridge system and should be able to register the effects of damage to each component on the overall bridge system. Therefore, in this study a global cumulative damage index is presented for the damage assessment of a bridge system by considering its component damage measures, namely:

$$DI_G = \sum \alpha_{ci} DI_{ci} \tag{7}$$

where DI_G is the damage index of the overall bridge system, DI_{ci} is the damage index of component i , which is calculated using Eq. (6), and α_{ci} is defined as the ratio of the energy dissipated by the component i to the total energy dissipated by the bridge system. It is expressed by:

$$\alpha_{ci} = \frac{E_{hi}}{\sum E_{hi}} = \frac{E_{hi}}{E_{hT}} \tag{8}$$

In Eq. (8), E_{hi} is the amount of energy dissipated by component i , and $\sum E_{hi}$ is the energy dissipated by the overall bridge system, which is calculated as the sum of the energy dissipated by all components. According to Eq. (7), the global cumulative index calculates the damage to an overall bridge as a linear combination of the weighted damage indices of its components (Fig. 1). As shown in Section 2, the values of DI_{ci} are in a range between 0 and 1 (Tables 4–5). According to Eq. (8), the values of α_{ci} are obtained in a range of 0–1. Therefore, the amount of the global cumulative damage index for a bridge system also is calculated to be in a range between 0–1. A damage value of zero means no damage occurs and a damage value of 1 indicates structural collapse.

4 Bridge models

In this paper, six multi-span continuous RC bridges, including box-girder and I-girder bridges with unequal and equal pier heights, are designed in accordance

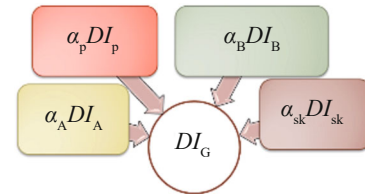


Fig. 1 Global cumulative damage index framework

Table 4 Strain-based damage levels of RC bridge piers (Mahboubi and Shiravand, 2019a)

Damage state	Damage description	Strain limits*	Damage index
DS-0	No damage	-	$DI < 0.1$
DS-1	Slight First cracking of concrete, Yielding of longitudinal bar	$\epsilon_{ctu} \leq \epsilon_{cover} < \epsilon_{ccu}$ $\epsilon_{sy} \leq \epsilon_s < \epsilon_{bb}$	$0.1 \leq DI < 0.2$
DS-2	Moderate Spalling of cover concrete	$\epsilon_{cover} \geq \epsilon_{ccu}$ $\epsilon_{sy} \leq \epsilon_s < \epsilon_{bb}$	$0.2 \leq DI < 0.7$
DS-3	Extensive Buckling of longitudinal bars	$\epsilon_s \geq \epsilon_{bb}$ $\epsilon_{ccore} < \epsilon_{ccu}$	$0.7 \leq DI < 0.9$
DS-4	Complete Crushing of core concrete	$\epsilon_{ccore} \geq \epsilon_{ccu}$	$0.9 \leq DI < 1$

*Note: ϵ_{ctu} : ultimate tensile strain of concrete, ϵ_{cover} : cover concrete strain, ϵ_s : steel strain, ϵ_{sy} : yield strain of steel, ϵ_{bb} : buckling strain of steel, ϵ_{ccore} : core concrete strain

Table 5 Damage levels of bridge bearings (Mahboubi and Shiravand, 2019c)

Damage state	Damage description	Damage Index
DS-0	Prior to sliding	$0 \leq DI < 0.2$
DS-1	Sliding	$0.2 \leq DI < 0.7$
DS-2	Failure	$0.7 \leq DI \leq 1$

with the AASHTO Guide Specifications for LRFD Bridge Design (2010). The properties of the bridges are presented in Table 6. Note that these bridges are selected from the most used RC bridge classes to consider various configuration and geometrical characteristics, including a varying number of spans, deck widths, column heights, bent types (single/multi-column bent), and bearing types. The bridges are designed using concrete that has a compressive strength of 25 MPa; the steel reinforcement yield strength is considered to be 400 MPa. As observed, bridges B-1, B-2, B-3, B-4 and B-5 have equal spans, whereas bridge B-6 has three unequal spans, which are 65 and 110 m long. Moreover, as shown in Table 6, the bridge models B-1, B-2, B-5 and B-6 are supported on piers and abutments with elastomeric bearings (Isolator), whereas bridge B-3 is supported on lead rubber bearings (LRB). Bridge B-4 is an integral bridge with single-column bents and has three unequal piers. In addition, bridges B-1 to B-5 employ circular columns, and bridge B-6 has rectangular columns. The general layout of RC bridges is displayed in Fig. 2.

5 Finite element modeling

Three-dimensional models of the bridges are generated using the Open System for Earthquake Engineering Simulation (OpenSees) program. Fiber-discretized, nonlinear beam-column elements are used for modeling columns. The cross-section of the bridge columns is divided into fiber cells with respect to their geometrical characteristics and the number of steel bars. Nonlinear material properties with specific stress-strain relationships are assigned to three different regions: unconfined concrete, confined concrete, and longitudinal steel reinforcements. General finite element models of the bridges are displayed in Fig. 3. In this paper, the OpenSees Concrete02 model is used, and the compressive strength and strain for the confined and unconfined concrete are defined based on the Mander *et al.* (1988) model. The steel reinforcements are simulated using the OpenSees reinforcing steel material model. The length of the plastic hinge in the columns is estimated in accordance with the

equation recommended by the Caltrans Seismic Design Criteria (2010), which considers the effects of strain localization and softening. The columns are assumed to be fixed at the soil foundation in all six rotational and translational directions. Rigid links are used to connect the columns to the bent beam or the solid diaphragm in the case of multi-column bents and provide moment and force transformation between the members of the bent. The deck is expected to remain elastic during seismic loadings and is modeled with equivalent elastic beam-column elements. The deck elements are connected to the bearing nodes on the bents or abutments, using rigid links at each end of the deck. Bearings are modeled using two-node link elements with a finite length, in accordance with the actual height of the bearings, considering P-delta effects. Bilinear hysteretic behavior of the elastomeric bearings (EB) and LRBs is defined using the models presented in Mahboubi and Shiravand (2019c) with respect to their geometrical and material properties, as provided in Table 6 and Fig. 3.

6 Verification of the finite element models

To validate the accuracy of the analytical model of the bridge piers, the experimental tests carried out by Kunnath *et al.* (1997) and Melek *et al.* (2003) are used. Kunnath *et al.* (1997) tested five circular bridge piers with flexural failure modes under cyclic loading by utilizing different displacement amplitudes. Melek *et al.* (2003) investigated the shear failure modes of RC bridge columns subjected to a constant axial load-repeated cyclic loading, which consisted of three cycles at each displacement level, with increasing drift levels of 0.1, 0.25, 0.75, 1, 1.5, 2, 3, 5, 7, and 10% (Melek *et al.*, 2003). Finite element models of tested specimens were then developed. The properties of experimental specimens are presented in Table 7. The lateral load-displacement responses of RC columns were validated against the experiment results (Fig. 4). As observed, the results show a good agreement between the fiber-based analysis and the experimental studies for flexural/bending and shear failure modes of RC columns.

Table 6 Properties of the bridges

Bridge	Number of span	Span length (m)	Deck width (m)	Column per bent	Column height (m)	Column dimensions (m)	Bearing stiffness (t-m)	Bearing type	T_1 (s)
B-1	3	30	12	3	10	$D = 2$	300	EB	0.98
B-2	5	30	12	2	5, 15	$D = 2$	300	EB	0.96
B-3	5	30	12	2	5, 15	$D = 2$	350	LRB	0.72
B-4	4	50	12	1	7, 14, 21	$D = 1.5, 2, 2.5$	-	-	1.23
B-5	3	20	25.1	6	15, 29	$D = 1.2$	280	EB	0.96
B-6	3	65, 110, 65	13.6	1	9	$a \times b = 4 \times 7$	485	EB	2.87

7 Ground motion suite and IDA

A suite of ground motions that is selected from the records developed for the PEER Transportation Research Program by Baker *et al.* (2011) is used as the input seismic load. The set consists of seven ground motions with magnitudes ranging from 6.1 to 7.6,

and the distance to rupture is less than 25 km. The characteristics of the ground motions are presented in Table 8. The response spectra of seven records, along with the median spectrum, are shown in Fig. 5. The median spectrum is compatible with soil type B, where the bridge is designed. To perform nonlinear incremental dynamic analysis (IDA), the peak ground acceleration

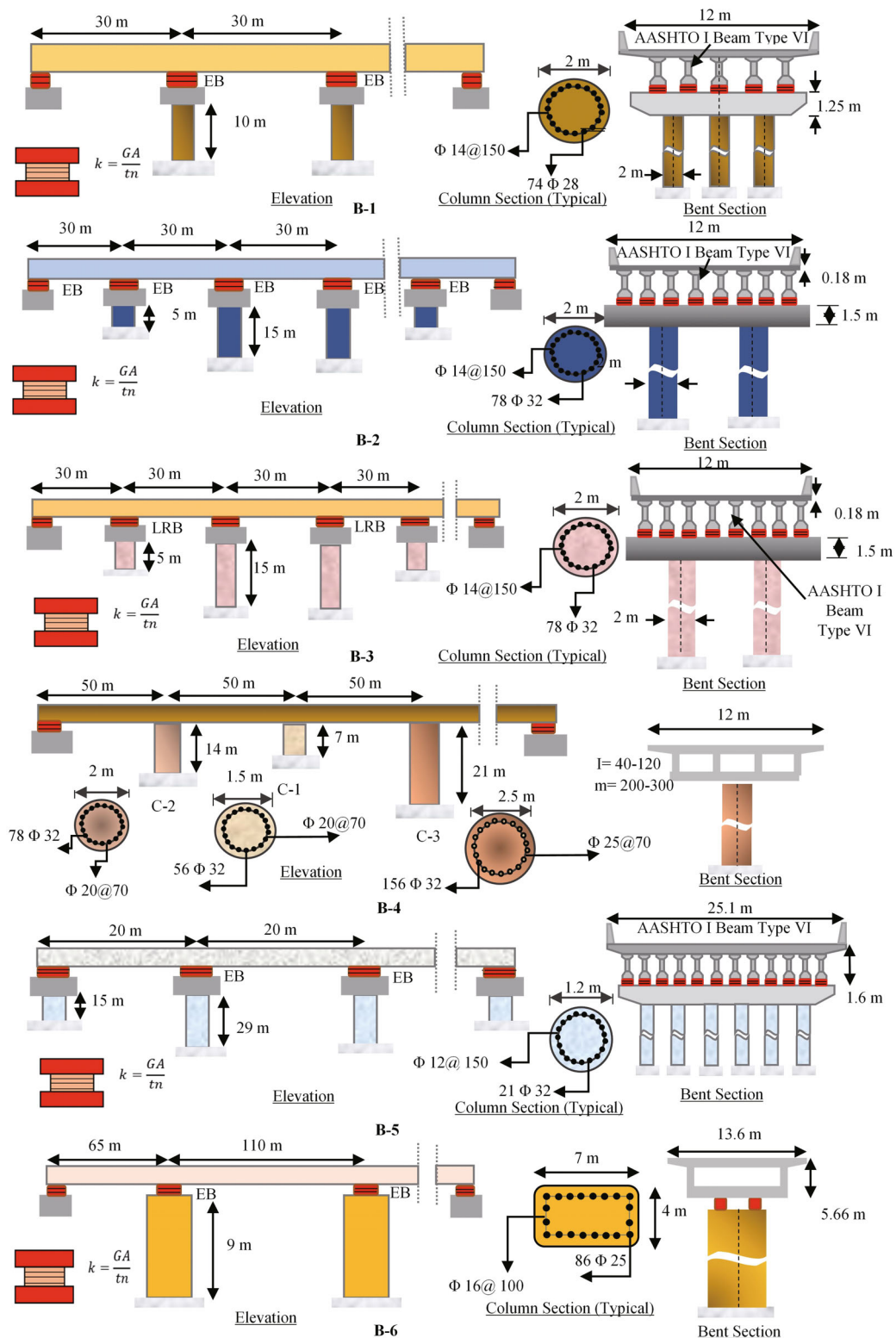


Fig. 2 Geometry and structural sections of the archetype bridges

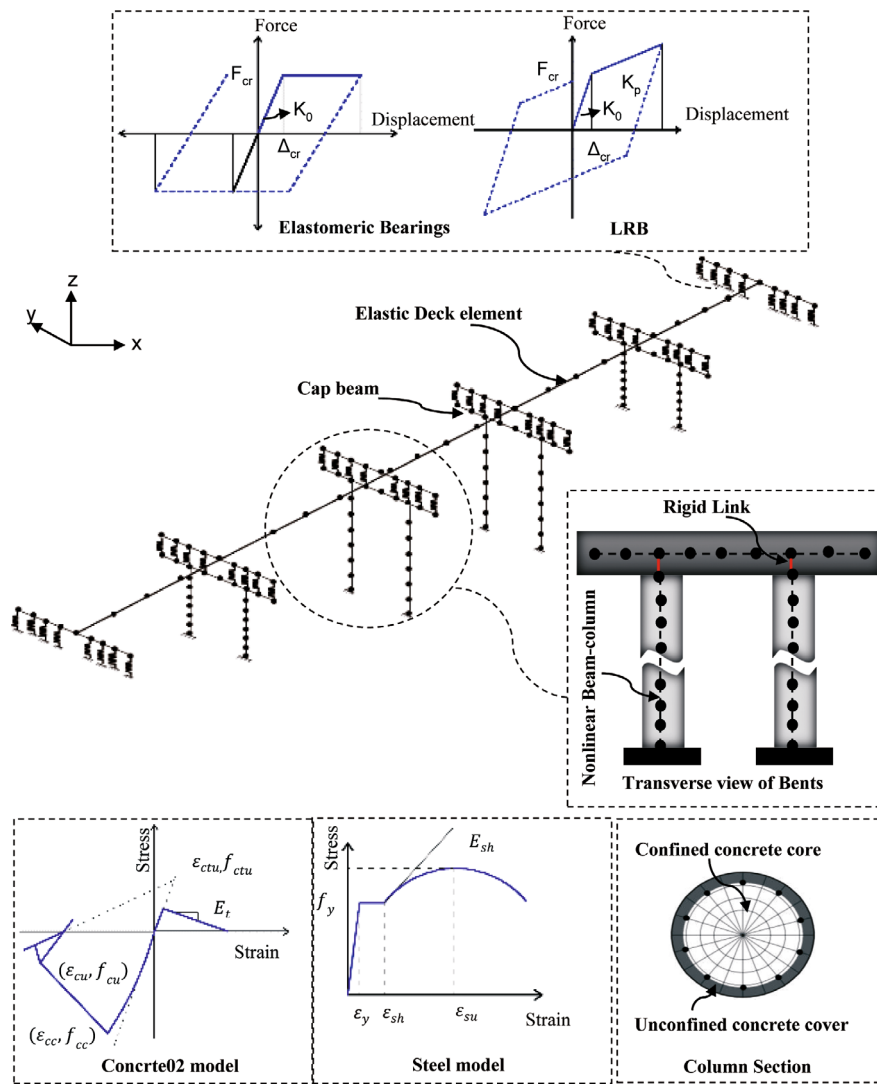


Fig. 3 General finite-element model of the RC bridge in OpenSees

Table 7 Details of prototype RC columns tested by Kunnath *et al.* (1997) and Melek *et al.* (2003)

Item	Kunnath <i>et al.</i> (1997)		Melek <i>et al.</i> (2003)	
	A2, A3	A4-A6	S30XI	S20HI
Longitudinal steel	21#3 (9.5mm)	21#3 (9.5mm)	8#8 (25.4 mm)	8#8 (25.4 mm)
Spiral/hoop	4 mm dia	4 mm dia	#3 (9.53 mm)	#3 (9.53 mm)
Spiral/hoop space	19 mm	19 mm	203.2 mm	203.2 mm
Concrete strength, f'_c	29 MPa	35.5 MPa	35 MPa	35 MPa
Longitudinal reinforcement steel yield strength, f_y	448 MPa	448 MPa	510 MPa	510 MPa
Transverse reinforcement yield strength, f_y	434 MPa	434 MPa	481 MPa	481 MPa
Column length	1.375 m	1.375 m	1.6764 m	1.6764 m
Axial load	806 kN	806 kN	1601 kN	1068 kN
Splice length	-	-	20 d_b	20 d_b

(PGA) of each record is scaled to the intensity measure of the design earthquake. Next, the PGAs of the records are scaled from 0.05 g and gradually increased with

increments of 0.05 g. For all bridge models, a nonlinear time-history analysis is performed at each step along the longitudinal axis of the bridges.

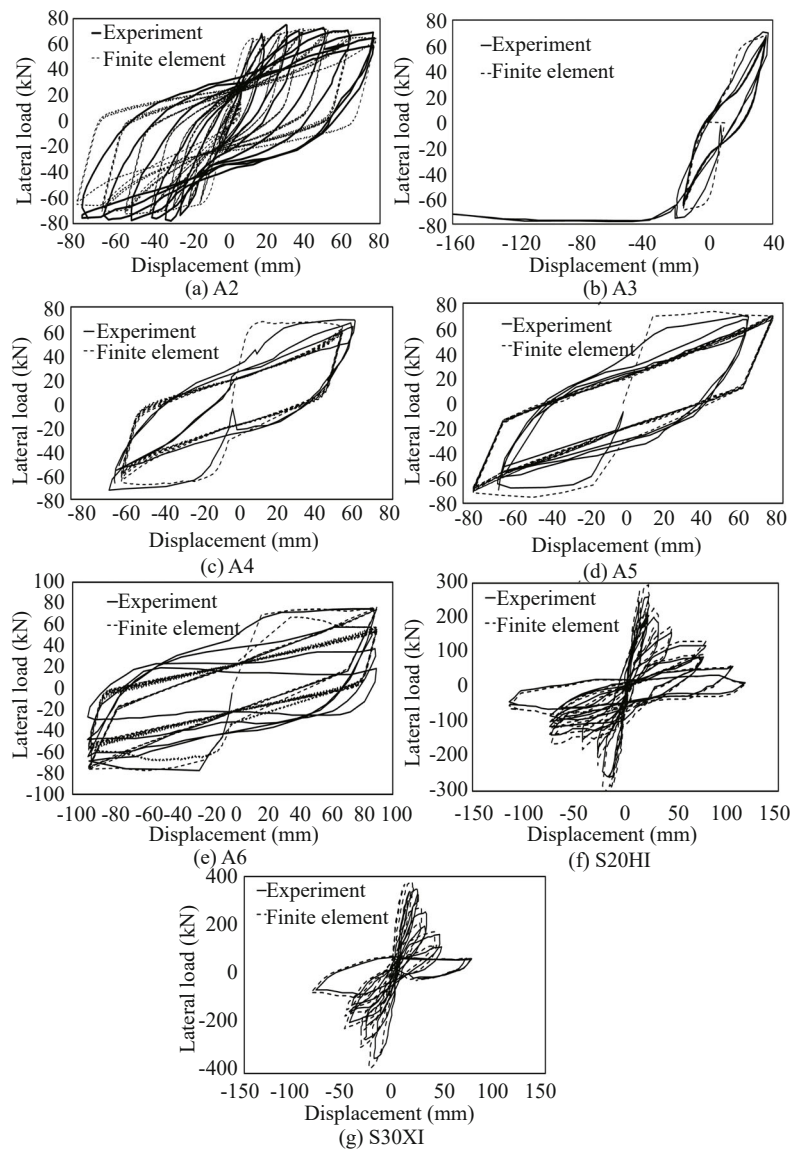


Fig. 4 Comparison of the lateral load-displacement behavior of RC columns in the experiment and the finite element

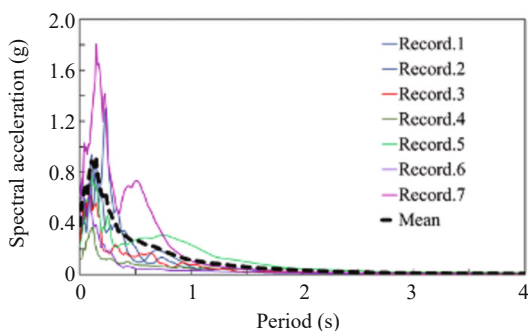


Fig. 5 Response spectra of seven earthquakes

8 Comparative study of damage indices

The values of the Park and Ang (1985), Hindi and Sexsmith (2001), and IEBD indices are calculated for the piers of bridges. Figure 6 shows the comparative damage curves of piers for the bridge model B-2 for all

earthquake records. As observed in Fig. 5, the increase in the PGA, raises the damage values of the piers obtained through all damage indices. However, the progression of the damage throughout all PGA values is different for the three damage models. For example, according to Fig. 6(a), in record No.1, for the short columns, the Hindi and Sexsmith (2001) damage model shows little damage prior to a PGA of 0.3 g, but increases rapidly to a damage value of 0.95, thereby representing a severe damage state, plus concrete crushing and bar buckling (Table 3) at a PGA of 0.5 g. On the other hand, the Park and Ang (1985) damage model and the IEBD index show a gradual increase from the beginning up to a PGA of 0.35 g and reach a damage value of 0.34 and 0.38, respectively. These damage values are correlated with severe cracking or localized spalling and spalling of cover concrete, as displayed in Tables 2 and 4. At a PGA of 0.5 g, the Park and Ang (1985) damage index is 0.75, representing concrete crushing and exposed

reinforcement, and the IEBD index is 0.78, showing extensive damage that is correlated to the buckling of steel bars. For the tall columns, the Park and Ang (1985) model indicates no damage prior to a PGA of 0.2 g and reaches a damage value of 0.68, corresponding to the severe damage state representing concrete crushing and exposed reinforcement at a PGA of 1 g. From this step, the Park and Ang (1985) damage index increases slowly to a damage value of 0.8 at a PGA of 2 g. In contrast, the Hindi and Sexsmith (2001) damage index provides a damage measure of 0.1, with a PGA of 0.3 g, then

suddenly increases and reaches a damage value of 0.78, with a PGA of 0.5 g, representing a severe damage state while corresponding to states of concrete crushing and reinforcement buckling. From this step, the damage index shows a rapid increase and reaches a damage value of 1, with a PGA of 1.1 g. Compared to other damage models, the IEBD index provides a smooth damage curve. The IEBD index gives a damage value of 0.19, with a PGA of 0.3 g, corresponding to slight cracking of cover concrete, and increases gradually to a damage value of 0.28, representing a moderate damage

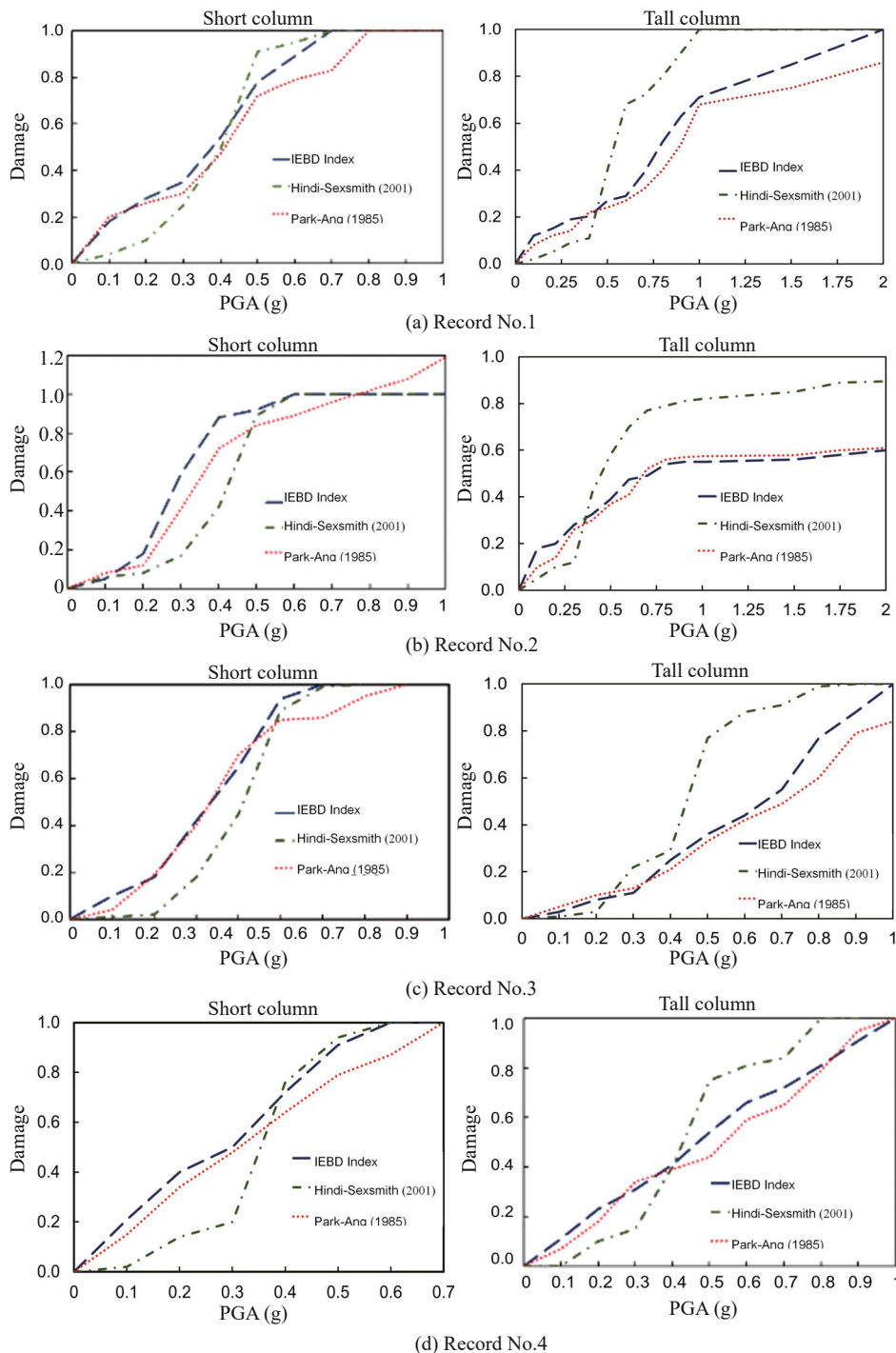


Fig. 6 Comparison of damage indices for piers of bridge model B-2 for all records

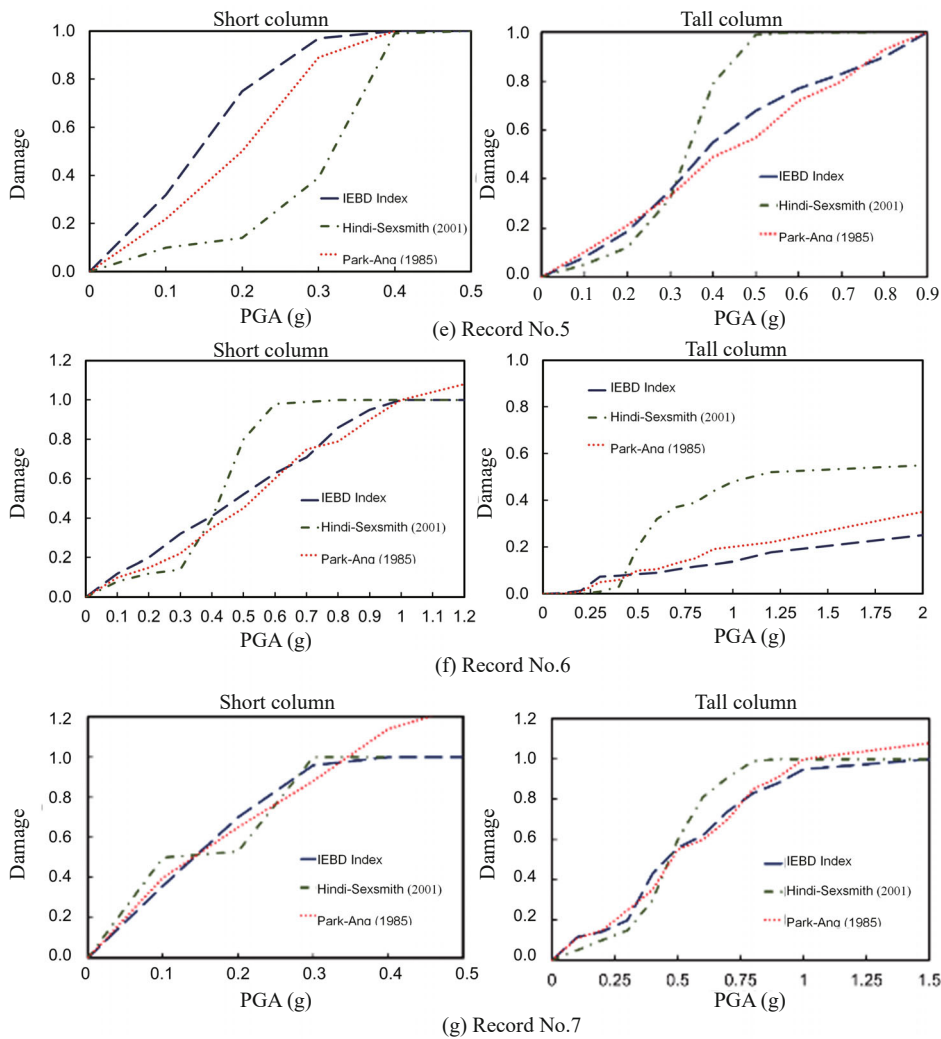


Fig. 6 Continued

state, with a PGA of 0.55 g. The increase in the PGA, boosts the damage measure to 0.78, with at a PGA of 1 g, and amplifies the damage level of the tall columns to the extensive level. The IEBD index increases to a damage value of 1, with a PGA of 2 g, representing complete damage to tall columns. As observed in Fig. 5, the Hindi and Sexsmith (2001) model shows severe early damage at lower PGA values compared to the Park and Ang (1985) and IEBD indices. In addition, the Park and Ang (1985) and IEBD indices provide a convincing gradual progression of different damage states and offer a good range of damage for different damage states, whereas the Hindi and Sexsmith (2001) damage index is found to underestimate the damage at low PGAs and to overestimate the damage at higher PGA values.

Average damage curves are developed for the bridge models to determine the damage measures for RC piers at two earthquake levels, including DBE and MCE (FEMA-P-752, 2009). DBE is defined as peak ground acceleration with a 10% probability of exceedance in 50 years, and MCE is the maximum considered earthquake with a 2% probability of exceedance in 50 years. Table 9 lists the obtained damage values for RC piers at the DBE

and MCE levels.

According to Table 9, for the bridge model B-1, the Park and Ang (1985) damage model lists damage values of 0.62 and 0.8, at the DBE and MCE levels, respectively. The IEBD index is 0.65 at DBE and 0.81 at the MCE level. In contrast, the damage values of piers provided by the Hindi and Sexsmith (2001) at the DBE and MCE levels are 0.19 and 0.9, respectively. Therefore, the IEBD index shows moderate damage and extensive damage states for bridge piers at the DBE and MCE levels, respectively. In contrast, the Park and Ang (1985) index indicates extensive damage to piers at both the DBE and MCE levels. On the other hand, the Hindi and Sexsmith (2001) model represents only slight damage at the DBE level and extensive damage level at the MCE level. For the B-2 bridge, the damage models provide higher damage values for the short columns, with higher stiffness at both the DBE and MCE levels. However, at DBE, the damage values provided by the Hindi and Sexsmith (2001) are very low in comparison to the damage measures obtained by the IEBD and Park and Ang (1985) indices. In general, according to Table 9, the damage measures of RC piers calculated by the

IEBD index, and the Park and Ang (1985) damage index are close and more reasonable compared to the damage values provided by the Hindi and Sexsmith (2001) model. The results show that the Hindi and Sexsmith (2001) index underestimates damage at the early stage and overestimates the extent of damage at a higher level of analysis.

9 Calculation of global energy-based damage index

9.1 Calculation of DI_B

To investigate the performance of the global cumulative damage index, the IEBD index is calculated for the piers and bearings of six bridge models. Then, the global cumulative damage index is calculated for the overall bridge systems. Since there are many responses for each bridge model with a different number of columns and bearings, only the average damage curves are presented here. The damage measures of RC piers, bearings, and the bridge system at the DBE and MCE level are identified in the damage curves. Figure 7 shows the average damage curves of the bearings for six bridge

models, calculated using the IEBD index in all records. For example, it is observed from Fig. 7 that the value of DI_B increases by increasing the PGAs. According to Fig. 7(a), for the B-1 bridge, the average values of DI_B under the DBE and MCE levels are calculated to be 0.76 and 0.83, respectively. This means that the bearings are at the failure damage level. In general, the IEBD index provides higher damage values for the bearings located on the short piers compared to those located on the long piers, which means that the bearings on the short piers are more vulnerable to earthquakes than those situated on the long piers. The stiffness of the short piers is higher than that of the tall piers, and the failure modes of the short piers at different damage states may occur before the tall piers reach their failure modes. Therefore, the bearings located on the short pier may act and reach the sliding state long before the ones located on the tall piers reach their sliding and failure damage states.

9.2 Calculation of DI_p

The average damage curves of RC piers are shown in Fig. 8. As observed, in the B-1 bridge, the average value of DI_p under the DBE is calculated to be 0.65, which

Table 8 Characteristics of input ground motion records

Record No.	Event	Year	Station	M_w	R (km)	PGA (g)	PGV (cm/s)	PGD (cm)
1	Chi-Chi	1999	CHY036	7.6	16.1	0.27	8.21	3.7
2	Chi-Chi	1999	CHY034	7.6	14.8	0.298	11.26	0.927
3	Imperial Valley	1979	Delta	6.5	22	0.236	6.33	21.95
4	Imperial Valley	1979	Calipatria Fire Station	6.5	24.6	0.123	6.25	2.15
5	Kocaeli	1999	Duzce	7.5	15.4	0.226	13.84	2.46
6	Mammoth Lakes	1980	Long Valley Dam	6.1	15.5	0.414	4.55	7.23
7	Northridge	1994	Sylmar - Converter	6.7	5.4	0.619	23	1.59

Table 9 Comparison of damage indices for RC piers of bridge models at DBE and MCE level

Bridge	Column	DBE						MCE					
		Park-Ang (1985)	DS [#]	Hindi-Sexsmith (2001)	DS	IEBD	DS	Park-Ang (1985)	DS	Hindi-Sexsmith (2001)	DS	IEBD	DS
B-1	C*	0.62	E	0.19	S	0.65	M	0.8	E	0.9	E	0.81	E
B-2	SC**	0.6	E	0.35	M	0.64	M	0.83	E	0.98	C	0.83	E
	TC***	0.25	M	0.26	S	0.25	M	0.40	M	0.71	E	0.44	M
B-3	SC	0.47	E	0.32	M	0.51	M	0.78	E	1	C	0.8	E
	TC	0.14	S	0.07	No	0.19	S	0.35	M	0.85	E	0.41	M
B-4	C-1	0.81	E	0.37	M	0.88	C	0.88	E	1	C	0.91	C
	C-2	0.32	M	0.08	No	0.38	M	0.7	E	0.99	E/C	0.71	E
	C-3	0.17	S	0.02	No	0.2	M	0.38	M	0.88	E	0.49	M
B-5	SC	0.39	M	0.22	M	0.41	M	0.67	E	0.96	E	0.7	E
	TC	0.25	M	0.14	S	0.26	M	0.41	E	0.91	E	0.56	M
B-6	C	0.15	S	0.18	S	0.38	M	0.54	E	0.99	E/C	0.63	M

Note: # Damage state; * Column; ** Short column; *** Tall column; S: Slight; M: Moderate; E: Extensive; C: Complete.

means that the piers are at the moderate damage level. Moreover, the average damage value corresponding to the MCE level is estimated to be 0.81, which shows that the piers are at the extensive damage level. In the case of the B-2 bridge, the average values of DI_p in the short and long piers under the DBE level are calculated to be 0.64 and 0.25, respectively. Therefore, the IEBD index shows that the columns are at the moderate damage level for the design earthquake. In addition, the average damage values of the short and long piers at the MCE level are calculated to be 0.83 and 0.44, respectively. Therefore, at the MCE level, the IEBD index predicts that the short piers are at the extensive damage level, whereas the damage level of the long piers are moderate at this stage. According to Fig. 8(c), for the B-3 bridge, the average values of DI_p of the short

columns corresponding to the DBE and MCE levels are estimated to be 0.51 and 0.8, respectively, which shows that the short columns are at the moderate damage level at DBE and are at the extensive damage state at the MCE level. Moreover, the average value of DI_p in the tall columns is calculated to be 0.19 under the DBE, which demonstrates that these columns are at the slight damage level. The corresponding damage value under the MCE is estimated to be 0.41, representing the moderate damage level. In the case of the B-4 bridge, it is observed from Fig. 8(d) that the average values of DI_p in columns C-1, C-2 and C-3 under the DBE are calculated to be 0.85, 0.38, and 0.24, respectively. Therefore, the IEBD index shows the short column, C-1, is at the extensive damage level, whereas C-2 and C-3 are at the moderate damage level at the DBE level. Moreover, the average damage

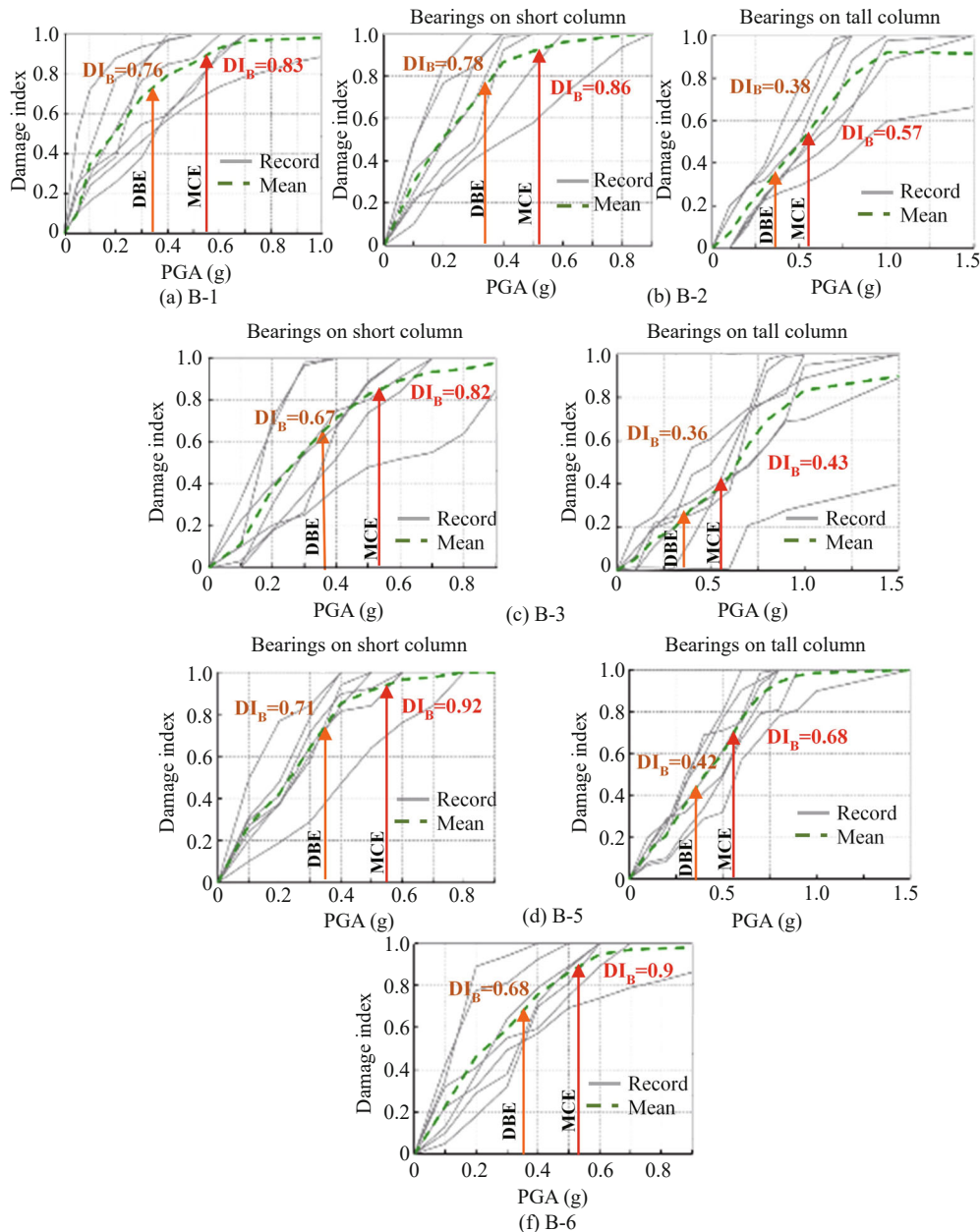


Fig. 7 Damage curves and the average value of DI_B for the bearings of six bridge models

values under the MCE for the columns C-1, C-2 and C-3, are equal to 0.91, 0.71 and 0.49, respectively. Therefore, column C-1 experiences complete damage and C-2 is at the extensive damage level, whereas C-3 is at the moderate damage level. For the B-5 bridge, at the DBE level, the average value of DI_p in the short columns is 0.41, representing the moderate damage level, whereas the corresponding damage value of the tall columns is calculated to be 0.26, representing the moderate damage level. In addition, at the MCE level, the average value of DI_p in the short columns is estimated to be 0.7, which means that the piers have entered the extensive

damage state. The corresponding damage value of the tall columns is equal to 0.56, which shows that these columns are at the moderate damage level at the MCE level. In the case of the B-6 bridge, the average values of DI_p under the DBE and MCE levels are calculated to be 0.38 and 0.63, respectively. Therefore, the IEBD index shows that the bridge piers are at the moderate damage level. Overall, the IEBD index provides higher values for the short columns compared to the tall columns in all bridge models, which confirms that the columns with higher stiffness experience higher damage at the DBE and MCE levels.

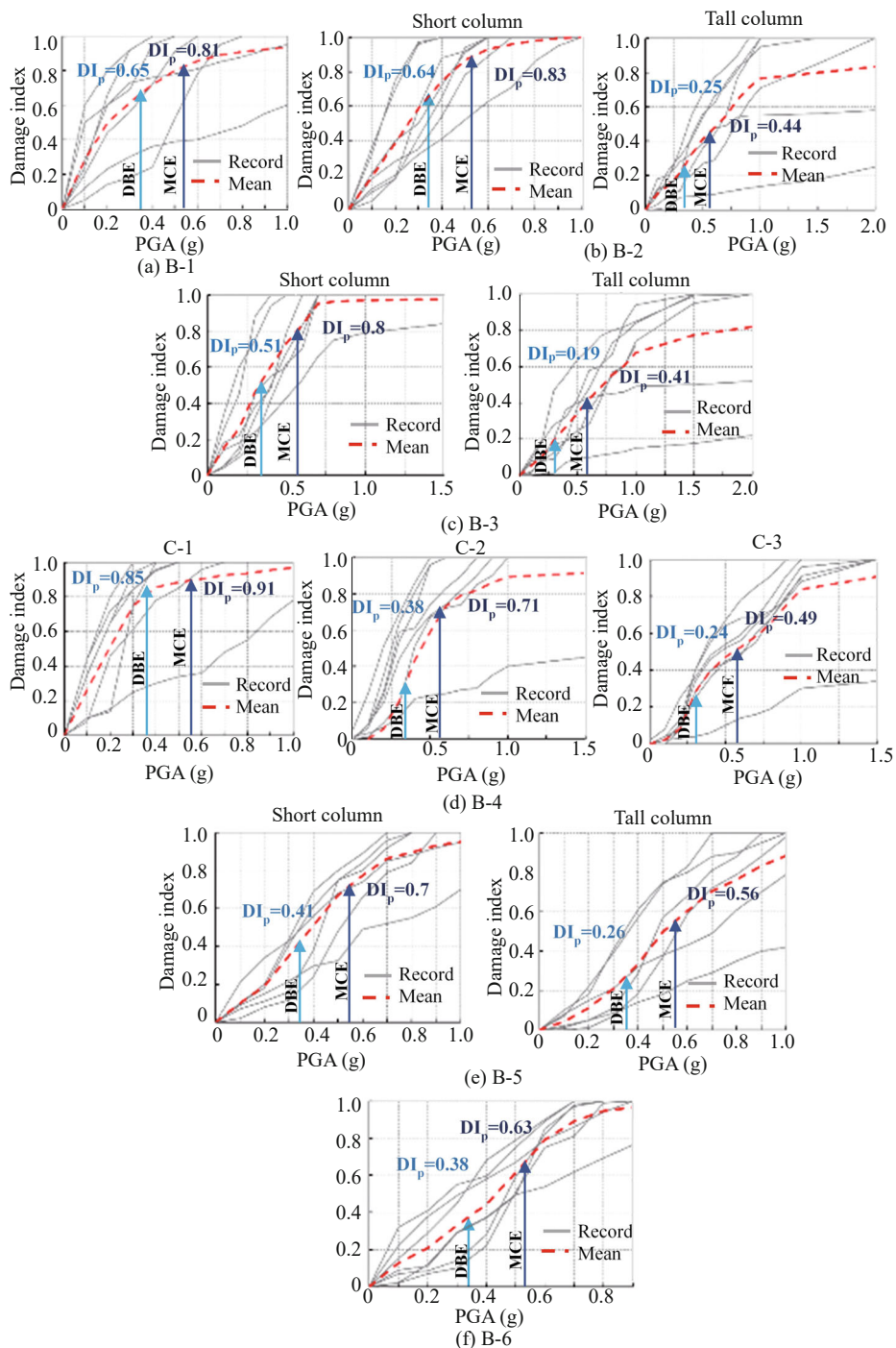


Fig. 8 Damage curves and the average value of DI_p for bridges B-2, B-3, B-4, B-5 and B-6

9.3 Calculation of α_{ci} and DI_G

To calculate the global damage index, the weight coefficients for the bridge bearings and columns are calculated using Eq. (8). As an example, the amount of dissipated energy from the bearings, E_{hb} ; the bridge piers, E_{hp} ; and the obtained values for α_B , α_P , DI_B , DI_P and DI_G at different increments of IDA for bridge model B-2 in record No.1 are presented in Table 10. As observed, the amount of for bearings located on the short columns and the ones situated on the tall columns are displayed in Table 10.

The global cumulative damage index, Eq. (7) calculated for bridge model B-2 is shown in Fig. 9. Note that points where the damage states of the piers and bearings are assumed to begin are indicated in Fig. 9 with circular markers. According to Fig. 9(a), in Record

No.1 the global cumulative damage index provides 12% damage to the B-1 bridge, at a PGA of 0.15 g. The damage values calculated for the bridge bearings show that the bearings located on the short piers are in the sliding damage state at this step, whereas the ones situated on the tall piers experience no damage. Moreover, at this step the short columns are at the slight damage level and no damage occurs in the tall columns. When the PGA reaches 0.25 g, the DI_G is equal to 30%. At this step, the bearings on the tall piers begin to slide, and the short and tall columns are at the moderate and slight damage levels, respectively. The increase in the PGA values raises the DI_G and at a PGA of 0.42 g, when the damage measure of the bridge system is 48%, the bearings on the short columns fail. The damage level of the short and tall columns is moderate at this stage. In addition, at a PGA of 0.49 g, in which the global cumulative damage index

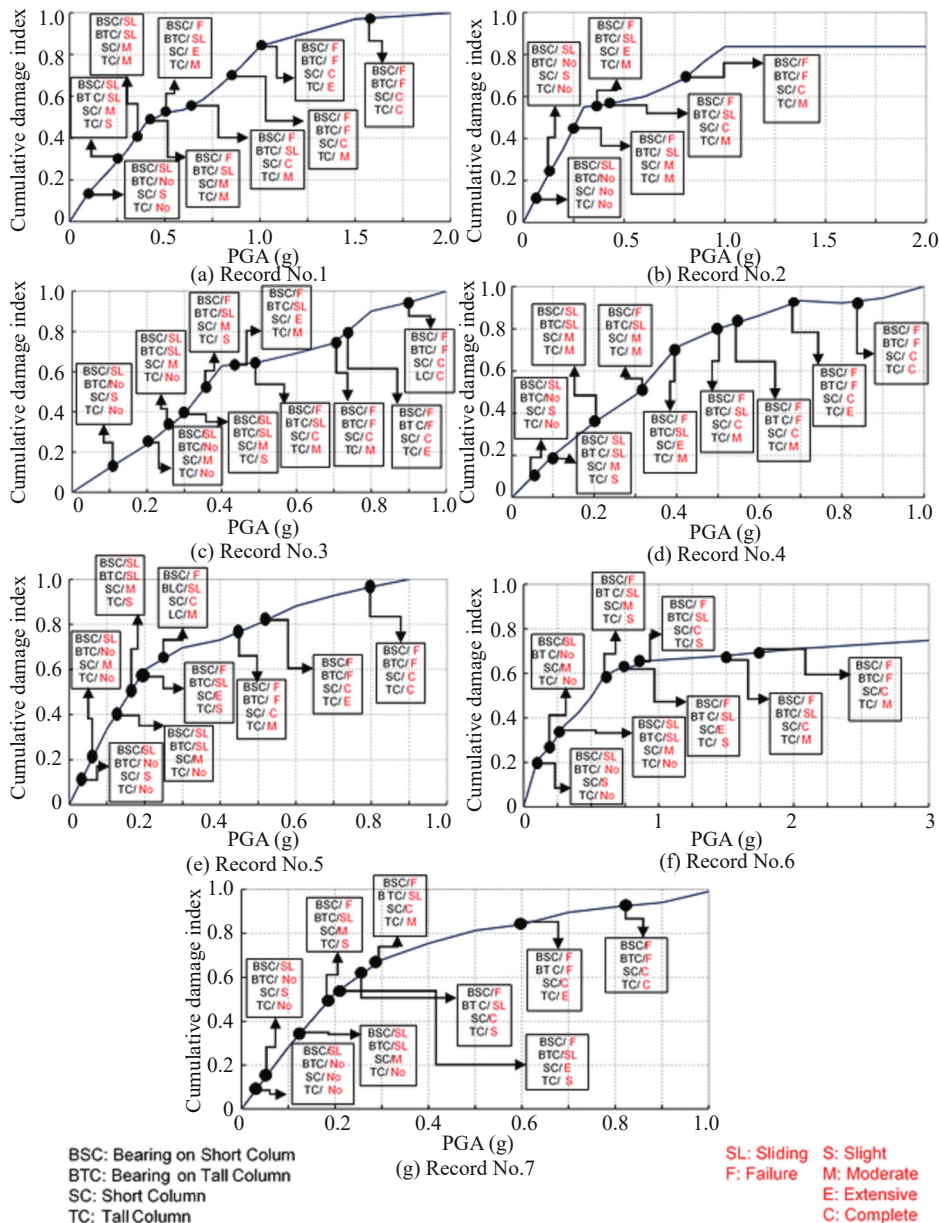


Fig. 9 Global cumulative damage index DI_G for bridge B-2

provides 51% damage to the bridge system, the short columns reach the extensive damage threshold. When the PGA value increases to 0.6 g, the global cumulative damage index shows 57% damage to the overall bridge system, which is correlated with a complete damage level for the short columns. According to Fig. 9(a), at a PGA of 0.85 g, the DI_G reaches 70%, at which point the bearings on the tall columns fail and the tall columns are still at the moderate damage level. At a PGA of 1g, when the DI_G is calculated to be 83%, all the bearings fail and the short columns are at the complete damage level, whereas the tall columns reach the extensive damage level limit. The DI_G increases by increasing the PGA of the record and reaches 98% at a PGA of 1.6 g, at which point the failure of tall columns starts. According to Fig. 9(b), in record No. 2, DI_G shows that damage to the bridge is about 23%, at a PGA of 0.15 g. The bearings on the short columns are at the sliding damage level and no damage is observed for the ones located on the tall columns. The IEBD index shows that the short columns are at the slight level at this step. At a PGA of 0.25 g, when the DI_G shows 42% damage to the system, the bearings on the short columns fail and the bearings on the tall columns are at the sliding damage level. The short and tall columns are at the moderate damage level. At a PGA of 0.34 g, the global cumulative damage index provides 56% damage to the

bridge system. At this stage, the short columns reach the extensive damage level. At a PGA of 0.43 g, the DI_G predicts 59% damage to the bridge, which is correlated with a complete damage level for the short columns and a moderate damage state for the long ones. When the DI_G indicates 70% damage, at a PGA of 0.8 g, all bearings fail and the short columns reach the complete damage state, whereas the tall columns are at moderate damage. The DI_G increases up to a PGA of 1g and remains constant up to the end of analysis, because the damage value of the tall columns remains at the moderate damage level and does not exhibit a considerable increase for the PGA, that is, in the range of 1-2 g.

Figure 10 shows the average cumulative damage index for all bridge models. As observed in Fig. 10(a), the average values of the DI_G for the bridge B-1 under the DBE and MCE levels are calculated to be 65% and 81%, respectively. In the case of the bridge B-2, the global cumulative damage index shows 58% damage to the bridge at the DBE level, whereas the DI_G exhibits 70% damage to the bridge at the MCE level. According to Fig. 10(c), the global cumulative damage index provides 41% damage to the bridge B-3 at the DBE level; at the MCE level, the global cumulative damage index predicts 62% damage to the overall bridge system. According to Fig. 10(d), the average damage value of

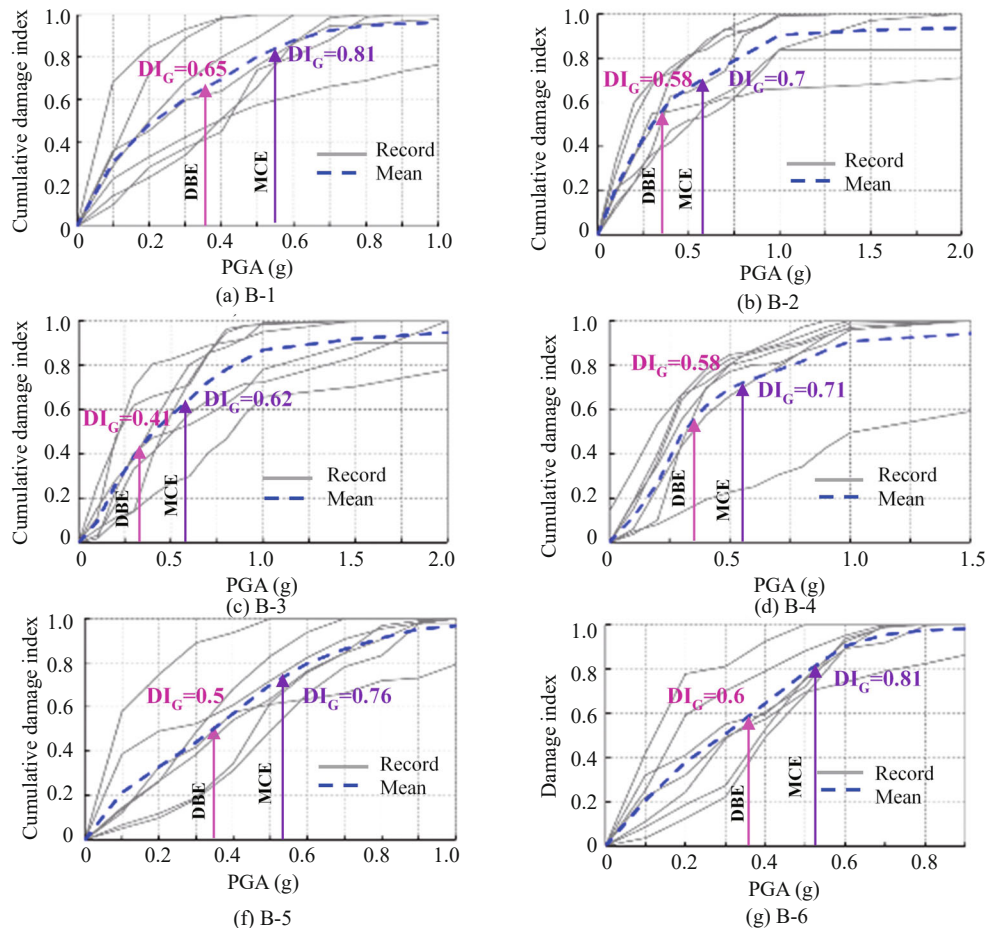


Fig. 10 Average value of the global cumulative damage index for all bridge models

Table 10 Values of α_B , α_P , DI_B , DI_P and DI_G at different PGAs for bearing and piers of bridge model B-2 in Record No. 1

Record No.1	Short Piers						Tall Piers						Bridge		
	Bearings			Column			Bearings			Column			E_{hT}	DI_G	
PGA	E_{hB}	$\alpha_B = \frac{E_{hB}}{E_{hT}}$	DI_B	E_{hP}	$\alpha_P = \frac{E_{hP}}{E_{hT}}$	DI_P	E_{hB}	$\alpha_B = \frac{E_{hB}}{E_{hT}}$	DI_B	E_{hP}	$\alpha_P = \frac{E_{hP}}{E_{hT}}$	DI_P			
0	0	0	0	0	0	0	0	0	0	0	0	0	0	0	0
0.1	76.8	0.174	0.10	264.82	0.6	0.18	48.55	0.11	0.0005	51.1986416	0.116	0.12	441.3	0.139	
0.2	3046.35	0.397	0.31	1734.19	0.226	0.28	1227.75	0.16	0.113	1665.14	0.217	0.15	7673.43	0.237	
0.3	7999.85	0.414	0.45	4173.84	0.216	0.35	2898.5	0.15	0.231	4251.13	0.22	0.19	19323.32	0.338	
0.4	1574.61	0.425	0.65	5370.66	0.145	0.54	7593.01	0.205	0.34	8333.8	0.225	0.203	22872.08	0.472	
0.5	17801.4	0.298	0.84	5197.05	0.087	0.78	22998.45	0.385	0.43	13739.33	0.23	0.27	59736.23	0.52	
0.6	10490.56	0.123	1	3240.98	0.038	0.89	50235.29	0.589	0.521	21322.28	0.25	0.29	85289.11	0.536	
0.7	12882	0.114	1	226	0.002	1	69156	0.612	0.592	30736	0.272	0.39	113000	0.584	
0.8	13442	0.094	1	143	0.001	1	91520	0.64	0.667	37895	0.265	0.52	143000	0.659	
0.9	9027	0.051	1	177	0.001	1	122130	0.69	0.764	45666	0.258	0.63	177000	0.742	
1	5325	0.025	1	0	0	1	154425	0.725	0.879	53250	0.25	0.71	213000	0.84	
1.5	421	0.02	1	0	0	1	336800	0.8	1	84200	0.2	0.85	421000	0.97	
2	0	0.01	1	0	0	1	428040	0.82	1	93960	0.18	1	522000	1	

bridge B-4 is calculated to be 58% at the DBE level, whereas the corresponding damage measure at the MCE level is 71%. For bridge B-5, the DI_G predicts 50% and 76% damage to the bridge system, at the DBE and MCE levels, respectively. For bridge B-6, the average values of the DI_G at the DBE and MCE levels are calculated to be 60% and 81%, respectively.

10 Summary and conclusions

This paper conducts a damage assessment study on six continuous-span RC bridges based on the IEBD index, which is a global cumulative damage index. First, a comparative study on the reliability of three damage indices is performed. This includes the Park and Ang (1985), the Hindi and Sexsmith (2001) and the IEBD models for the seismic damage assessment of RC bridge piers. Second, a global cumulative damage index for the damage evaluation of the overall bridge system based on the IEBD index is presented. The global cumulative damage index is defined as a combination of the component damage indices multiplied by the weight coefficients. The energy-based damage indices and the global damage index are calculated for six RC bridges under earthquake ground motions using IDA. Various damage levels of the bridges are evaluated at two DBE and MCE hazard levels. The results are summarized as follows:

- The IEBD index and the Park and Ang (1985) damage model show a gradual progression of damage and provide smoother damage curves compared to the Hindi and Sexsmith (2001) damage index. The Hindi and Sexsmith (2001) index underestimates the damage to RC piers at the early stages during loading cycles and overestimates the damage at higher PGAs. Therefore, the Hindi and Sexsmith (2001) model fails to predict

damage to RC bridge piers throughout dynamic analysis.

- The damage assessment results indicate that the damage values of the bearings at DBE and MCE levels are higher than damage indices obtained for the corresponding piers in all bridge models. This implies that the bridge bearings reach their failure modes, including sliding and failure, at lower PGA values compared to the bridge columns, which are located on them. Moreover, in bridge models with unequal piers, the bearings located on the short piers, which have higher stiffness values compared to the tall piers, are more vulnerable to earthquake excitations and reach the siding and failure damage states at lower PGA values in all records.

- The damage analysis results reveal that for all bridge models with unequal piers (B-2, B-3, B-4 and B-5), damage values of the short piers with higher stiffness levels are larger than the tall piers and consequently the short piers reach the extensive and collapse damage levels at lower PGA values. In addition, the IEBD index shows that at the DBE level, the bridge piers are mostly in the moderate damage state, with severe spalling of cover concrete. At the MCE level, the IEBD index shows that shorter columns with higher stiffness in bridge models B-2, B-3 and B-4 reach the extensive damage level, which corresponds to the buckling of the longitudinal bars, whereas damage to the tall columns is mostly moderate.

- The calculated values of show that when the PGA of the record is relatively low, the earthquake input energy has been mostly dissipated by the bridge bearings, up to the failure point, and after that the inelastic behavior of the columns mostly dissipates input energy.

- Damage estimation of the bridge system using the IEBD index of the components represents the effects of component damage regarding seismic-induced

damage to the overall bridge system at each point time during loading history, a finding not provided by any damage models. Moreover, incorporation of the damage measures using the weight coefficients that are defined in accordance with the energy dissipation capacity ratio of the components ensures that the effects of the inelastic behavior of all components at each time step throughout the loading are considered in a reliable manner.

- The global cumulative damage index provides damage measures in a range between 0 and 1. Value of the damage index equal to 1 indicates the collapse of the bridge system, which is correlated to the complete failure of the bearings and piers.

11 Recommendations for future work

There are some additional ideas that we would like to develop:

- It could be interesting to perform a damage analysis of the bridge models in two other directions, transverse and vertical, to develop damage curves and more precisely determine the damage levels of components and the overall system of the bridges.

- It could be useful to perform seismic damage analysis with larger numbers of ground motion records.

- The effects of the seismic behavior of other components such as abutments and shear keys can be investigated and added to the global cumulative damage index.

References

AASHTO (2010), *LRFD Bridge Design Specification*, American Association of State Highway and Transportation Officials, Washington DC, USA.

Babazadeh A, Burgueño R and Silva PF (2015), "Use of 3D Finite-Element Models for Predicting Intermediate Damage Limit States in RC Bridge Columns," *Journal of Structural Engineering*, ASCE, ISSN 0733-9445/04015012(11).

Baker J, Lin T, Shahi S and Jayaram N (2011), "New Ground Motion Selection Procedures and Selected Motions for the PEER Transportation Research Program," *Pacific Earthquake Engineering Research Center Report*.

Banerjee S and Shinozuka M (2008), "Experimental Verification of Bridge Seismic Damage States Quantified by Calibrating Analytical Models with Empirical Field Data," *Earthquake Engineering and Engineering Vibration*, 7(4): 383–393.

Bassam A, Iranmanesh A and Ansari F (2011), "A Simple Quantitative Approach for Post-Earthquake Damage Assessment of Flexure Dominant Reinforced Concrete Bridges," *Engineering Structures*, 33(12): 3218–3225.

Caltrans (2010), *Caltrans Seismic Design Criteria*

Version 1.6. Sacramento, CA: California Dept. of Transportation.

Calvi GM, Pavese A, Rasulo A and Bolognini D (2005), "Experimental and Numerical Studies on the Seismic Response of RC Hollow Bridge Piers," *Bulletin of Earthquake Engineering*, 3: 267–297.

Cardone D (2014), "Displacement Limits and Performance Displacement Profiles in Support of Direct Displacement-Based Seismic Assessment of Bridges," *Earthquake Engineering and Structural Dynamics*, 3: 1239–1263.

Chai TH, Romstad KM and Bird SM (1995), "Energy-Based Linear Damage Model for High-Intensity Seismic Loading," *Journal of Structural Engineering (ASCE)*, 121(5): 857864.

El-Bahy A, Kunnath SK, Stone WC and Taylor AW (1999), "Global Cumulative Seismic Damage of Circular Bridge Columns: Benchmark and Low-Cycle Fatigue Tests," *ACI Structural Journal*, 96(4): 633–641.

Erberik MA and Sucuoğlu H (2004), "Seismic Energy Dissipation in deteriorating Systems Through Low-Cycle Fatigue," *Journal of Earthquake Engineering and Structural Dynamics*, 33: 49–67.

FEME-P-752 (2009), *NEHRP Recommended Seismic Provisions*, Federal Emergency Management Agency of the Department of Homeland Security.

Goodnight JC, Kowalsky M and Nau J (2019), "Strain Limit States for Circular RC Bridge Columns," *Earthquake Spectra*.

Guo Zongming, Zhang Yaotingm, Lu Jiezhi and Fan Jian (2016), "Stiffness Degradation-Based Damage Model for RC Members and Structures Using Fiber-Beam Elements," *Earthquake Engineering and Engineering Vibration*, 15(4): 697–714.

Hachem MM, Stephan AM and Moehle JP (2003), "Performance of Circular Reinforce Concrete Bridge Columns Under Bidirectional Earthquake Loading," *PEER Rep. 2003/06*, Pacific Earthquake Engineering Research Center College of Engineering University of California, Berkeley, CA, USA.

Hindi RA and Sexsmith RG (2001), "A Proposed Damage Model for RC Bridge Columns Under Cyclic Loading," *Earthquake Spectra*, 17(2): 261–290.

Hindi RA and Sexsmith RG (2004), "Inelastic Damage Analysis of Reinforced Concrete Bridge Columns Based on Degraded Monotonic Energy," *Journal of Bridge Engineering*, 9(6): 326–332.

Iranmanesh A and Ansari F (2014), "Energy-Based Damage Assessment Methodology for Structural Health Monitoring of Modern Reinforced Concrete Bridge Columns," *Journal of Bridge Engineering (ASCE)*, 19(8): A4014004.

Jara JM, Lopez MG, Jara M and Olmos BA (2014), "Rotation and Damage Index Demands for RC Medium-Length Span Bridges," *Engineering Structures*, 75: 205–217.

- Krawinkler H and Zohrei M (1983), "Global Cumulative Damage in Steel Structure Subjected to Earthquake Ground Motions," *Computer and Structures*, **16**(1-4): 531–541.
- Kunnath SK, El-Bahy A, Taylor AW and Stone WC (1997), "Global Cumulative Seismic Damage of Reinforced Concrete Bridge Piers," Buffalo, NY: State Univ. of New York at Buffalo, National Center for Earthquake Engineering Research.
- Lehman DE and Moehle JP (2000), "Seismic Performance of Well-Confined Concrete Bridge Column," *PEER Report No.1998/01*, Berkeley, CA: Pacific Earthquake Engineering Research Center, College of Engineering, Univ. of California, USA.
- Mahboubi S and Kioumars M (2021), "Damage Assessment of RC Bridges Considering Joint Impact of Corrosion and Seismic Loads: A Systematic Literature Review," *Construction and Building Materials*, **295**: 123662. <https://doi.org/10.1016/j.conbuildmat.2021.123662>
- Mahboubi S and Shiravand MR (2019a), "A Proposed Input Energy-Based Damage Index for RC Bridge Piers," *Journal of Bridge Engineering (ASCE)*, **24**(1): 1–19.
- Mahboubi S and Shiravand MR (2019b), "Failure Assessment of Skew RC Bridges with FRP Piers Based on Damage Indices," *Engineering Failure Analysis*, **99**: 153–168.
- Mahboubi S and Shiravand MR (2019c), "Seismic Evaluation of Bridge Bearings Based on Damage Index," *Bulletin Earthquake Engineering*, **17**: 4269–4297.
- Mander JB, Chen S and Peckan G (1994), "Low Cycle Fatigue Behavior of Semi-Rigid Top and-Seat Angle Connections," *Engineering Journals (AISC)*, **31**(3): 111–122.
- Mander JB, Priestley MJN and Park R (1988), "Theoretical Stress Strain Model for Confined Concrete," *Journal of Structural Engineering*, **114**(8): 1804–1826.
- Nielson BG and DesRoches R (2007), "Analytical Seismic Fragility Curves for Typical Bridges in the Central and Southeastern United States," *Earthquake Spectra*, **23**(3): 615–633.
- Oskoui E, Taylor T and Ansari F (2019), "Method and Monitoring Approach for Distributed Detection of Damage in Multi-Span Continuous Bridges," *Engineering Structures*, **189**: 385–395.
- Padgett JE, Nielson BG and DesRoches R (2008), "Selection of Optimal Intensity Measures in Probabilistic Seismic Demand Models of Highway Bridge Portfolios," *Earthquake Engineering and Structural Dynamic*, **37**: 711–725.
- Park YJ and Ang AH (1985), "Mechanistic Seismic Damage Model for Reinforced Concrete," *Journal of Structural Engineering*, **111**: 722–739.
- Powell GH and Allahabadi R (1998), "Seismic Damage Prediction by Deterministic Methods: Concepts and Procedures," *Earthquake Engineering and Structural Dynamics*, **16**(5): 719–734.
- Roy A, Bhattacharya G and Roy R (2017), "Maximum Credible Damage of RC Bridge Pier Under Bi-directional Seismic Excitation for All Incidence Angles," *Engineering Structures*, **152**: 251–273.
- Seyed Ardakani SM, Saiid Saiidi M and Somerville P (2021), "Residual Drift Spectra for RC Bridge Columns Subjected to Near-Fault Earthquakes," *Earthquake Engineering and Engineering Vibration*, **20**(1): 193–211. <https://doi.org/10.1007/s11803-021-2014-y>
- Shiravand MR and Rasouli M (2019), "Effects of Substructure Mass Participation on Natural Period of Multi-Column Base Isolated Bridges," *Structures*, **20**: 88–104.
- Sun Zhiguo, Li Hongnan, Bi Kaiming, Si Bingjun and Wang Dongsheng (2017), "Rapid Repair Techniques for Severely Earthquake-Damaged Circular Bridge Piers with Flexural Failure Mode," *Earthquake Engineering and Engineering Vibration*, **16**(2): 415–433.